Article

Carbodiimide Synthesis via Ti-Catalyzed Nitrene Transfer from Diazenes to Isocyanides

Evan P. Beaumier, Meghan E. McGreal, Adam R Pancoast, Ryan Hunter Wilson, James T Moore, Brendan Joseph Graziano, Jason D. Goodpaster, and Ian A. Tonks

ACS Catal., **Just Accepted Manuscript** • DOI: 10.1021/acscatal.9b04107 • Publication Date (Web): 11 Nov 2019

Carbodiimide Synthesis via Ti-Catalyzed Nitrene Transfer from Diazenes to Isocyanides

Evan P. Beaumier, Meghan E. McGreal, Adam R. Pancoast, R. Hunter Wilson, James T. Moore, Brendan J. Graziano, Jason D. Goodpaster,* Ian A. Tonks*

Department of Chemistry, University of Minnesota - Twin Cities, 207 Pleasant Street SE, Minneapolis, Minnesota 55455, United States

ABSTRACT: Simple Ti imido halide complexes such as $[Br_2Ti(N^tBu)py_2]_2$ are competent catalysts for the synthesis of unsymmetrical carbodiimides via Ti-catalyzed nitrene transfer from diazenes or azides to isocyanides. This is the only example of catalytic nitrene transfer to isocyanides where diazenes have been employed as the nitrene source. Both alkyl and aryl isocyanides are compatible with the reaction conditions, although product inhibition with sterically unencumbered substrates sometimes limits the yield when diazenes are employed as the oxidant. The reaction mechanism has been investigated both experimentally and computationally, wherein a key feature is that product release is triggered by electron transfer from an η^2-carbodiimide to a Ti-bound azobenzene. This ligand-to-ligand redox buffering obviates the need for high-energy formally Ti^{II} intermediates, and provides further evidence that substrate and product "redox noninnocence" can promote unusual Ti redox catalytic transformations.

Keywords: *Titanium, Nitrene Transfer, Isocyanide, Carbodiimide, Redox Catalysis, Redox Non-Innocence*

INTRODUCTION

Transition metal-catalyzed nitrene transfer reactions are efficient and highly atom economical routes for the synthesis of nitrogen-containing molecules.[1–4] There are many examples of transition metal-catalyzed nitrene transfer using Rh,[5–8] Ag,[9] and late transition metal porphyrin complexes.[10–12] However, there are significantly fewer examples of catalytic nitrene transfer reactions with early transition metals. This is partly because the reactivity of high-valent early transition metal imido (M≡NR) complexes is dominated by redox-neutral reactions such as [2+2]-cycloaddition and 1,2-addition.[13–16] Recently, we have demonstrated that azobenzene can be used as an oxidant in formal nitrene transfer reactions that stem from initial Ti≡NR and alkyne [2+2]-cycloaddition.[17–24] In an effort to expand the use of azobenzene as a nitrene source in catalytic reactions beyond [2+2] cycloadditions, we sought to use isocyanides as migratory insertion partners with Ti≡NR fragments *en route* to catalytic carbodiimide formation.

Carbodiimides are used as dehydration reagents in chemical synthesis,[25–27] polymer materials,[28,29] and dyes.[30–33] Unsymmetrical carbodiimides are often synthesized via dehydration of ureas[34,35] or dehydrosulfurization of thioureas.[36,37] However, nitrene transfer to isocyanides is an attractive alternative as it provides a potentially more direct and atom economical alernative.[38-52]

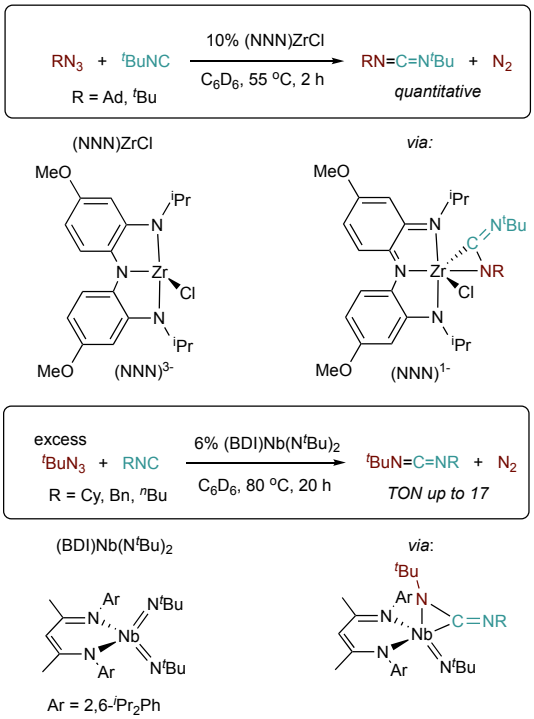

Figure 1. Examples of catalytic carbodiimide formation using early transition metals. Top: Redox-active ligands enable oxidation with a Zr catalyst. Bottom: π-overloading yields Nb (*bis*)imidos that are active toward isocyanide insertion. Both proceed through key η^2-carbodiimide adducts.

Although there are several examples of isocyanide migratory insertions into high-valent early transition metal imidos,[53–57] there are only two examples of catalytic carbodiimide formation (Figure 1). In one case, Heyduk used a redox-active (*tris*)amide ligand capable of reversible reduction from an NNN^{-1} "quinonate" to an NNN^{3-} catecholate on Zr (NNN^{3-} = bis(2-isopropylamido-4-methoxyphenyl)amide).[47] A similar approach for catalytic nitrene carbonylation has been demonstrated by Wolczanski using a redox-active diamide-diimine ($dadi^{2-}$) ligand capable of reversible reduction to an ene-tetraamide $dadi^{4-}$ ligand ($dadi^{2-}$ = {-CH=N(1,2-C_6H_4)N(2,6-^{i}Pr$_2$-C_6H_3)}$_2$).[58] In the second case, Arnold and Bergman have accomplished catalytic carbodiimide formation using a π-loading strategy with (BDI)Nb(N^{t}Bu)$_2$ (BDI = 2,6-diisopropylphenyl-β-diketiminate),[46] where the two imido ligands competitively π-donate into the Nb center, providing a more reactive imido. Both examples of catalytic carbodiimide formation use azides as the terminal oxidant (Figure 1). Herein, we report that catalytic nitrene transfer from diazenes to isocyanides can be achieved with simple Ti imido halide complexes, demonstrating that the redox-noninnocence of the substrates and products are enough to stabilize otherwise high-energy low-valent intermediates.

RESULTS AND DISCUSSION

We first explored the reaction of ^{t}BuNC with PhNNPh under catalytic conditions similar to those in our previous Ti-catalyzed nitrene transfer reactions (Table 1).[19] Reaction of 2.2 equiv. *tert*-butylisocyanide with PhNNPh and 10 mol % **1a** in $PhCF_3$ at 115 °C for 24 hours afforded 1-*tert*-butyl-3-phenylcarbodiimide (**2a**) in 59% yield (Table 1, entry 1). The more electron-deficient catalysts **1b**, **1c**, and **1d**, which we previously found to be more active for Ti redox catalysis,[20] gave yields of 77%, 85%, and 69%, respectively (Table 1, entries 2-4). Given that the yields of reactions with **1b**-**1d** were comparable, further reactions were carried out using **1d** because it is cheaper and more stable than **1c**, and easier to synthesize and more soluble than **1b**. Increasing the concentration of ^{t}BuNC from 0.724 M to 0.988 M and using 5 mol % **1d** generated **2a** in 85% yield (entry 5). In each entry where *tert*-butylisocyanide was used, small amounts of ^{t}BuNCN^{t}Bu (**3**) were generated, with yields ranging from 8-13%. The formation of this side product will be discussed later.

Both 2,6-xylylisocyanide and cyclohexylisocyanide gave poor yields of **2a'** and **2a"**, respectively, even after prolonged reaction times (entries 6-9). These low yields could be a result of the formation of stable *tris*(RNC) adducts (*vide infra*) or from product inhibition. Reactions of PhNNPh with ^{t}BuNC catalyzed by **1d** in the presence of approx. 10% of either **2a'** or **2a"** resulted in severe rate inhibition (SI, Figure S55), indicating that the low yields in entries 6-9 may partially be a result of product inhibition. In contrast, bulkier **2a** exhibits weaker product inhibition (SI, Figure S54), leading to productive catalysis.

Table 1. Exploration of catalyst and isocyanide scope.[a]

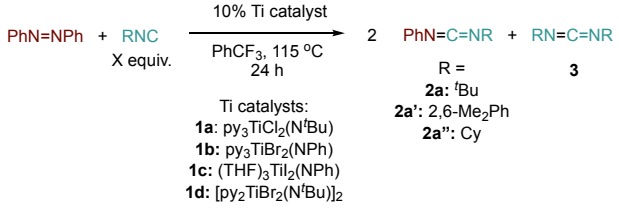

Entry	R	Equiv. RNC	Ti cat.	% yield **2**	% yield **3**
1	^{t}Bu	2.2	**1a**	59	13
2	^{t}Bu	2.2	**1b**	77	8
3	^{t}Bu	2.2	**1c**	85	9
4[b]	^{t}Bu	2.2	**1d**	69	10
5[b]	^{t}Bu	3	**1d**	85	12
6[b]	2,6-Me$_2$Ph	3	**1d**	<1[d]	-
7[b,c]	2,6-Me$_2$Ph	3	**1d**	3[d]	-
8[b]	Cy	3	**1d**	<1[d]	-
9[b,c]	Cy	3	**1d**	<1[d]	-

a: Reaction conditions: 0.165 mmol PhNNPh, 0.362 mmol RNC (entries 1-4) or 0.495 mmol RNC (entries 5-9), 0.0165 mmol Ti catalyst (10 mol %). Yields were determined via No-D ^{1}H NMR with respect to 1,3,5-trimethoxybenzene as an internal standard. *b*: 5 mol % [py$_2$TiBr$_2$(N^{t}Bu)]$_2$ (10 mol% [Ti]). *c:* Reaction time = 144 h. *d*: Yields

were determined via GC-FID with respect to 1,3,5-trimethoxybenzene as an internal standard.

Next, the azoarene scope was investigated in C_6D_5Br, which gave a slightly lower NMR yield of **2a** than when using $PhCF_3$. Table 2, entry 1). A variety of electronically donating and withdrawing diazenes were examined, most of which provided the corresponding 1-*tert*-butyl-3-arylcarbodiimides **2a**-**2f** in good yields (Table 2, entries 1-6,). 4,4'-bis(trifluoromethyl)-azobenzene provided **2f** successfully, albeit only in 43% yield (Table 2, entry 6). Notably, this same diazene is completely unreactive in Ti-catalyzed nitrene transfer to alkynes for pyrrole formation.[19] Several *ortho*-substituted derivatives were explored as well, yielding the corresponding 1-*tert*-butyl-3-arylcarbodiimides in good yields for *o*-Me (**2g**) and *o*-Et (**2h**) (Table 2, entries 7-8), though the yield decreased notably with bulkier *o*-^{i}Pr substitution (**2i**, Table 2, entry 9). Again, ^{t}BuNCN^{t}Bu (**3**) was generated in all reactions, with yields ranging from 6-11%. These reactions can also be easily scaled: a 1 g scale reaction of azobenzene with ^{t}BuNC resulted in 72% isolated yield of **2a** (Table 2, entry 1).

Table 2. Diazene scope for $[py_2TiBr_2(N^tBu)]_2$ (**1d**)-catalyzed carbodiimide formation.[a]

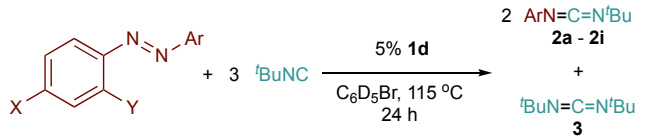

Entry	X	Y	Product	% yield **2**	% yield **3**
1	H	H	**2a**	79 (72%)[c]	9 (3%)[c]
2	Me	H	**2b**	75	11
3	F	H	**2c**	70	8
4	Cl	H	**2d**	70	8
5	OCF_3	H	**2e**	71	7
6[b]	CF_3	H	**2f**	44	7
7	H	Me	**2g**	69	8
8	H	Et	**2h**	70	6
9	H	^{i}Pr	**2i**	42	6

a: Reactions conditions: 0.165 mmol PhNNPh, 0.495 mmol ^{t}BuNC, 0.00825 mmol $[py_2TiBr_2(N^tBu)]_2$ (5 mol %) in 0.5 mL C_6D_5Br. Yields were determined via ^{1}H NMR with respect to 1,3,5-trimethoxybenzene as an internal standard. *b*: 8 h reaction time; significant product decomposition occurs between 8 and 24 h. *c:* Isolated yield, reaction conditions: 5.49 mmol PhNNPh, 16.5 mmol ^{t}BuNC, 0.275 mmol $[py_2TiBr_2(N^tBu)]_2$ (5 mol %) in 20 mL $PhCF_3$ at 115 °C for t = 40 h.

Given the product inhibition seen with less bulky isocyanides, we envisioned that increasing the steric bulk of the nitrene source would allow for productive catalysis. The results of reactions of adamantyl azide (AdN_3) with various isocyanides catalyzed by **1d** are shown in Table 3. Here, the less sterically encumbered CyNC and 2,6-xylylNC (Table 3, entries 2-3) also give satisfactory yields of the unsymmetric carbodiimide products **4b** and **4c**, respectively. In addition to the steric encumberance of the adamantyl group, the stronger coordinating ability of AdN_3 compared to PhNNPh may also promote productive catalysis through outcompeting product inhibition or isocyanide coordination.

Table 3. $[py_2TiBr_2(N^tBu)]_2$ (**1d**)-catalyzed carbodiimide synthesis from AdN_3.[a]

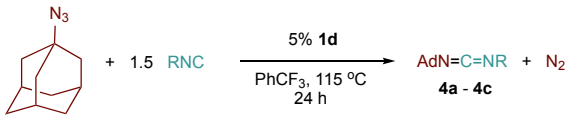

Entry	R	Product	% yield
1	^{t}Bu	**4a**	63
2	Cy	**4b**	55
3	2,6-Me_2Ph	**4c**	86

a: Reaction conditions: 0.280 mmol AdN_3, 0.420 mmol RNC, 0.0140 mmol **1d** (5 mol %) in 1 mL $PhCF_3$. Isolated yields.

Although 1,1-insertion of early metal imidos into isocyanides has been demonstrated previously,[53–57] we next wanted to explore the mechanism of this reaction in more detail to understand how ligands, substrates, and products could synergistically affect the Ti redox process. Compared to previous catalytic examples where overt redox-noninnocent ligands were used to promote catalysis,[47] here the critical factors promoting redox catalysis are less clear. Same excess kinetic measurements indicated both product inhibition and catalyst decomposition over the course of the reaction, precluding a full kinetic investigation (SI, Figures S53 and S54). Further preliminary kinetic studies indicated very complex and intractable reaction orders. Thus, we turned to DFT calculations to give further insight into the potential speciation and energetics of catalysis.

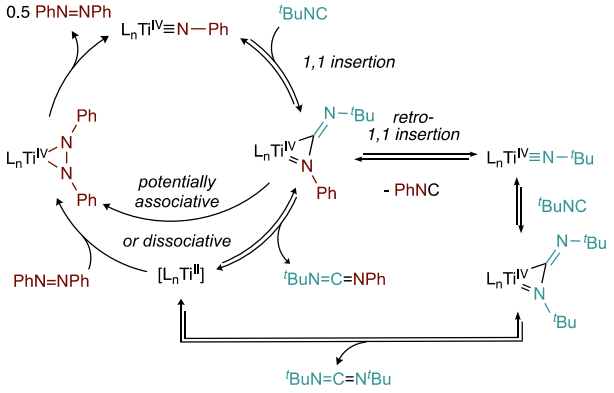

Figure 2. Proposed mechanism for carbodiimide formation using isocyanides and diazenes catalyzed by **1d**.

Combined experimental and DFT results are consistent with the mechanism of 1-*tert*-butyl-3-phenylcarbodiimide (**2a**) formation proposed in Figure 2. First, an isocyanide coordinates to the Ti imido, which then undergoes a 1,1-migratory insertion into the Ti-imido bond, generating an η^2-carbodiimide. Next, substitution of the carbodiimide ligand with PhNNPh occurs via either an associative or

dissociative manner to give the product carbodiimide and an η^2-hydrazido, which disproportionates[19,59–62] to regenerate the Ti imido and 0.5 equiv. PhNNPh. The formation of ^{t}BuNCN^{t}Bu *via* retro-1,1 insertion will be discussed later (*vide infra*).

A significant challenge in studying these simple Ti halide catalytic systems is the potential for speciation. Previous DFT analysis of Ti-catalyzed nitrene transfer in the [2+2+1] synthesis of pyrroles showed large energetic changes based on ligand speciation.[20] Here, pyridine, isocyanide, azobenzene, or carbodiimide could potentially act as a spectator ligand in some (or all) steps of catalysis. As a result, we undertook a study of the effect of various ligand combinations across the entirety of the reaction profile for the synthesis of **2a** from ^{t}BuNC and PhNNPh (Figure 3). The 6 spectator ligand combinations investigated were a single pyridine (**red**), two pyridines (**blue**), pyridine/isocyanide (**green**), 1 isocyanide (**grey**), two isocyanides (**black**), and azobenzene (**orange**). In all possible ligand combinations, pathways matching the steps shown in Figure 2 were found to be lowest energy.

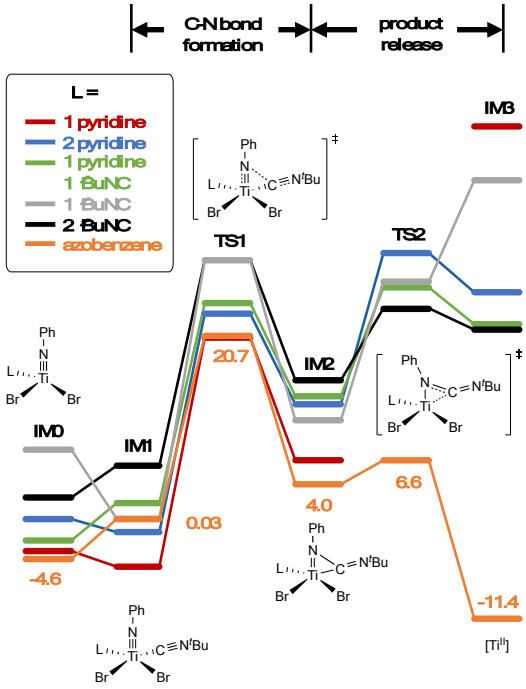

Figure 3. Free energy (kcal/mol) reaction profiles for various ligand combinations for isocyanide amination catalysis leading to **2a** from ^{t}BuNC and PhNNPh. Free energy values listed are for L = azobenzene. All intermediate and transition state energies are relative to the IM0 intermediate bearing two pyridine ancillary ligands. For all other free energy values, see Table 4.

Table 4. Free energies (kcal/mol) for intermediates and transition states of various ligand combinations shown in Figure 3. The lowest-energy species for each intermediate/transition state is bolded and italicized.

	IM0	IM1	TS1	IM2	TS2	IM3
1 py	-3.7	***-5.5***	***19.8***	6.7	--	44.5
2 py	0.0	-1.6	23.2	12.8	30.1	25.8
1 py and 1 ^{t}BuNC	-2.6	1.7	24.5	13.9	26.2	22.1
1 ^{t}BuNC	7.8	-0.08	29.3	11.0	26.8	38.4
2 ^{t}BuNC	2.3	6.1	29.3	15.6	23.8	21.4
PhNNPh	***-4.6***	0.03	20.7	***4.0***	***6.6***	***-11.4***

The ancillary ligand combination significantly impacts the energetics of catalysis (Table 4). A key observation is that many possible ligand combinations are close in energy, and thus multiple species may be participating in catalysis. Most importantly, however, is that coordination of azobenzene (Figure 4, **orange**) significantly lowers the barrier for all steps of catalysis—in particular, there is a strong effect on product release. As will be discussed below, this is due to two factors: (1) azobenzene is not a strong σ-donor ligand, resulting in an electron-deficient Ti that facilitates 1,1-migratory insertion in **TS1**; and (2) azobenzene is a strongly π-accepting ligand and can directly accept the pair of electrons in **TS2** that were formerly backbonding into the C=N π* of the η^2-carbodiimide ligand, circumventing the formation of a discrete Ti^{II} species proceeding from **TS2** to **IM3**. This π-acceptor character can be observed in the computed azobenzene N-N bond lengths: from **IM0** through **TS2**, the N-N bond length of 1.25 Å is consistent with an N=N double bond, but upon carbodiimide dissociation it is lengthened to 1.40 Å in **IM3**.

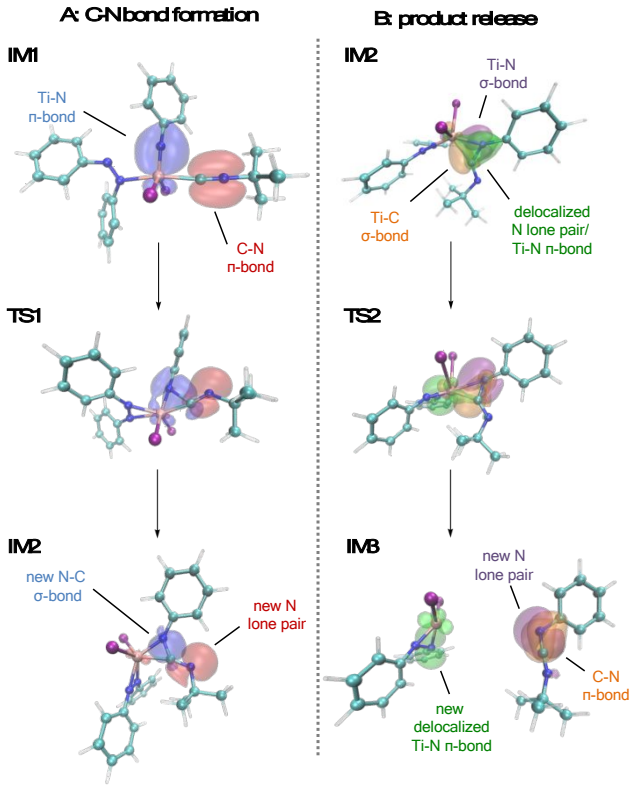

Figure 4. (A) IBOs of the reactant (IM1), transition state (TS1), and product (IM2) in the first step of ^{t}BuNC amination with PhNNPh. The IBOs show the Ti-N π-bond forming a new N-C σ bond (blue orbital) and the C-N π-bond forming a new N lone pair (red orbital). (B) IBOs from the intermediate (IM2), transition state (TS2), and final dissociated product (IM3). The IBOs show the Ti-N σ bond breaking to form a new N lone pair (purple orbital), the Ti-C σ bond breaking to form a new C=N π-bond (orange orbital), and a delocalized N lone pair/Ti-N π-bond transferring through the titanium to form a new Ti-N π-bond with azobenzene (green orbital).

Next, intrinsic bond orbital (IBO) analysis was carried out on the reaction pathway with ligated azobenzene (Figure 4). IBOs provide a connection between DFT calculations and the curved arrow formalism[63,64], and give a simple view of electron flow during a reaction. For the 1,1-insertion step (Figure 4a, **IM1** proceeding through **TS1** to **IM2**) an electron pair on one of the Ti≡NR π-bonding orbitals (blue) attacks the isocyanide C=N π* orbital, forming the new C=N bond and pushing an electron pair on to N (red). This type of Ti≡N π to C-N σ bond-forming event is reminiscent of our recent report on [2+2+1] pyrrole formation,[20] where C-N bond formation occurs through π orbitals in an electrocyclization event. For the product release step (Figure 4b, **IM2** proceeding through **TS2** to **IM3**), the azobenzene π-acceptor character is very important. Here **TS2** involves 3 critical orbital changes: (1) breaking of the ^{t}BuNC-Ti σ bond to form the product carbodiimide C=N π bond (orange), (2) breaking of the Ti=NPh π bond to form a new π backbond with azobenzene (orange), and (3) breaking of the Ti-NPh σ-bond to form the carbodiimide N lone pair (purple).

Natural Bond Order (NBO)[65,66] analysis further supports the importance of the azobenzene π-acceptor character. Previously, we have benchmarked formal Ti oxidation states by examining the occupancy of the Ti 3dz^2 orbital through NBO analysis, where occupancies closer to 0.4 correlate well to formal Ti^{IV}, and occupancies closer to 0.6 correlate well to formal Ti^{II}.[20] The 3dz^2 occupancies of all intermediate ligand combinations, as well as for the 1,1-insertion and product dissociation transition states **TS1** and **TS2**, is presented in Table 5. Here, structures with weaker donors (pyridine, azobenzene) have lower 3dz^2 occupancy in **TS1** (correlating to a more oxidized Ti metal center) and thus undergo more facile 1,1-insertion with isocyanide. Additionally, structures with π-accepting ligands (isocyanide, azobenzene) have lower 3dz^2 occupancy in **TS2**, making ligand loss more facile as the building charge on the Ti^{II} fragment can be simultaneously buffered by the π-accepting ligands. Importantly, Ti remains significantly more oxidized when azobenzene is a ligand because the weak N=N π bond is an excellent π-acceptor—in fact, by NBO analysis of the 3dz^2 occupancy, Ti remains close to the +4 oxidation state throughout catalysis when azobenzene is bound.

Azobenzene's synergistic "redox-neutral" buffering of electron density serves the same purpose as an ancillary redox noninnocent ligand, and was previously proposed by Wang for several other Ti redox catalytic reactions.[67,68] Interestingly, previous computations for pyrrole product release from Ti^{II} in the related catalytic formal [2+2+1] synthesis of pyrroles does not require this type of buffering.[20] While the reasons for this difference are currently unclear, a contributing factor could be the stability of the released product: in the case of pyrrole release, reformation of the aromatic ring (loss of Ti-pyrrole backbonding) could be enough of a driving force to eject Ti^{II} even in the absence of azobenzene as a redox buffer; on the contrary, in carbodiimide synthesis (and the related carboamination reactions calculated by Wang[68]), formation of a single C=N π bond is likely not enough of a driving force to eject free Ti^{II}. Nonetheless, it is also important to note that the other (non-azobenzene bound) pathways are low enough in energy (~25 kcal/mol, Table 4) that they also may contribute to the overall reaction rate to some extent, and that azobenzene is not absolutely critical for catalysis.

Table 5. NBO-derived Ti 3dz^2 occupancies of calculated intermediates and transition states from Figure 3. Values closer to 0.4 are assigned as formally Ti^{IV} while closer to 0.6 (bold, italics) are assigned as formally Ti^{II}.

	IM0	IM1	TS1	IM2	TS2	IM3
1 py	0.32	0.31	0.36	0.45	--	***0.76***
2 py	0.31	0.31	0.35	0.44	***0.65***	***0.63***
1 py and 1 ^{t}BuNC	0.30	0.32	0.36	0.46	***0.56***	***0.62***
1 ^{t}BuNC	0.32	0.31	0.39	0.45	***0.58***	***0.67***

2 ^{t}BuNC	0.31	0.32	0.37	0.47	***0.57***	***0.62***
PhNNPh	0.31	0.31	0.35	0.44	0.40	0.39

Next, we investigated the formation of the "nitrene scrambled" ^{t}BuNCN^{t}Bu byproduct **3** that is observed in all reactions with ^{t}BuNC. Notably, when using catalysts **1b** and **1c** (Table 1, entries 2 and 3; Figure 5), ^{t}BuNCN^{t}Bu was still formed in 8% and 9% yield, respectively. These results demonstrate that ^{t}BuNCN^{t}Bu formation is not solely generated from stoichiometric reaction of the ^{t}Bu imido group of the precatalyst.

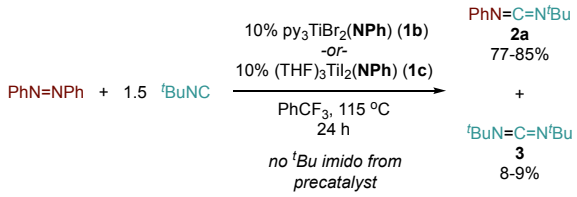

Figure 5. Formation of ^{t}BuNCN^{t}Bu (**3**) using catalytic **1b** or **1c** demonstrates that this sideproduct is not solely formed from Ti(N^{t}Bu) precatalyst activation.

A process in which the nitrene fragments are formally scrambled could reasonably occur through either an isocyanide metathesis or carbodiimide metathesis pathway (Figure 6). In an isocyanide metathesis, a Ti≡NPh imido undergoes a 1,1-insertion with ^{t}BuNC to form an η^2-carbodiimide. Instead of undergoing ligand dissociation to liberate the carbodiimide product, the η^2-carbodiimide undergoes *retro*-1,1 insertion to liberate PhNC and a Ti≡N^{t}Bu imido, which can react further with ^{t}BuNC to yield ^{t}BuNCN^{t}Bu (Figure 6, top). In a carbodiimide metathesis pathway, an equivalent of ^{t}BuNCNPh product undergoes [2+2] cycloaddition with a Ti≡NPh imido, ultimately liberating PhNCNPh and the Ti≡N^{t}Bu imido necessary to yield ^{t}BuNCN^{t}Bu (Figure 6, bottom). There is only a single report of d^0 metal imido promoted isocyanide metathesis.[46] On the contrary, there are both stoichiometric[69–71] and catalytic[72–75] examples of carbodiimide metathesis with d^0 metal imidos, although dihalide Ti imidos have been shown to be poor catalysts for this transformation.[74] Experimentally, we have not observed either of the expected byproducts of these pathways, PhNC or PhNCNPh, in significant quantities under catalytic conditions, although control experiments indicate that both pathways may be operable (SI, Figure S52).

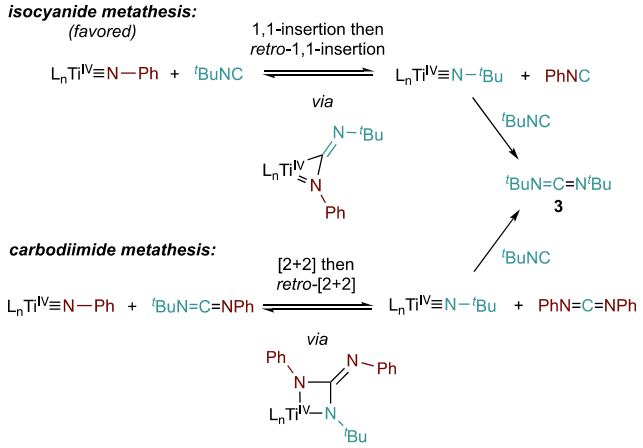

Figure 6. Possible mechanisms leading to formation of Ti *tert*-butyl imido moieties responsible for catalytic production of ^{t}BuNCN^{t}Bu (**3**).

Figure 7 shows the DFT-calculated free energy profiles of isocyanide metathesis (blue) and carbodiimide metathesis (red) catalyzed by $py_2TiBr_2(N^tBu)$. In the isocyanide metathesis pathway (Figure 7, blue), the first steps of the reaction are identical to productive carbodiimide formation (Figure 3, **IM0** through **IM2**), where ^{t}BuNC first coordinates to the Ti≡NPh imido followed by 1,1-insertion of isocyanide into the Ti-imido bond, yielding an η^2-carbodiimide (**IM2**). From here, the η^2-carbodiimide Ti complex rearranges to the adjacent C=N^{t}Bu π-bond, resulting in an isomeric η^2-carbodiimide structure (**IM3-ICM**) of almost equal energy to **IM2**. **IM3-ICM** next undergoes rate-determining (27.2 kcal/mol) *retro*-1,1 insertion, yielding a Ti≡N^{t}Bu imido with a bound PhNC ligand (**IM4-ICM**), which can dissociate to yield the free Ti≡N^{t}Bu imido **IM5-ICM**. In the carbodiimide metathesis pathway (Figure 7, red), the starting Ti≡NPh imido **IM0** undergoes [2+2] cycloaddition with PhNCN^{t}Bu, yielding the guanadinate **IM2-CM**. **IM2-CM** then undergoes rate-determining (34.7 kcal/mol) *retro*-[2+2] cycloaddition in the opposite manner, yielding the Ti≡N^{t}Bu imido **IM3-CM** with the expulsion of PhNCNPh.

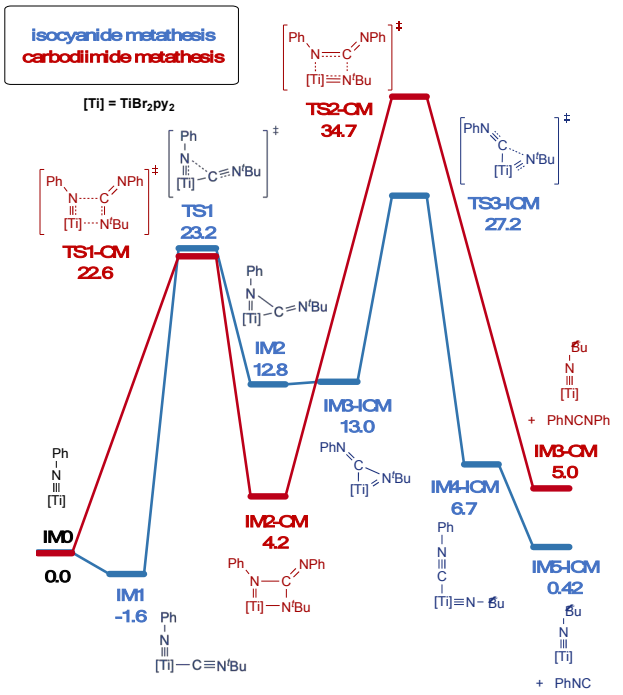

Figure 7. Free energy profiles of possible mechanisms leading to formation of Ti *tert*-butyl imido moieties responsible for catalytic production of ^{t}BuNCN^{t}Bu (**3**). Blue: isocyanide metathesis with ^{t}BuNC. Red: carbodiimide metathesis with PhNCN^{t}Bu (**2a**). All intermediate and transition state energies are relative to the IM0 intermediate bearing two pyridine and two bromide ancillary ligands.

Comparing the scrambling pathways, the rate-determining barrier for isocyanide metathesis (**TS3-ICM**, 27.2 kcal/mol) is significantly lower than for carbodiimide metathesis (**TS2-CM**, 34.7 kcal/mol), indicating that isocyanide metathesis is the likely major pathway of scrambling. The computed rate-determing step for productive unsymmetrical carbodiimide formation (Table 4, **TS2**, 2 py, 30.1 kcal/mol) is slightly higher than TS3-ICM for isocyanide metathesis. However, these calculations were performed with 2 ancillary pyridine ligands, and upon ligand exchange to azobenzene the productive redox pathway to unsymmetrical product is much lower in energy (Table 2, **TS2**, 1 azobenzene 6.6 kcal/mol) Since isocyanide and carbodiimide metatheses are redox neutral pathways, coordination of azobenzene will not significantly change the barrier for **TS3-ICM** or **TS2-CM** (by analogy, as seen in Figure 3, and Table 4, the barrier for **TS1** changes < 5 kcal/mol moving from py_2 ligation to azobenzene ligation). Thus, productive catalysis will in most cases kinetically outcompete isocyanide metathesis if azobenzene is present, accounting for the low yields of the symmetrical ^{t}BuNCN^{t}Bu byproduct.

In conclusion, we have demonstrated that catalytic nitrene transfer to isocyanides using diazenes or azides can be accomplished with the simple Ti imido halide complex $[Br_2Ti(N^tBu)py_2]_2$. DFT analysis of the reaction profile suggests that during the initial steps of isocyanide coordination to Ti and 1,1 migratory insertion, the ligand environment around Ti is somewhat ambiguous, showing similar barriers for several possible ligand combinations. Alternatively, the carbodiimide dissociation step likely proceeds while Ti is bound to a diazene ligand in an overall associative ligand exchange process, given that the barrier for carbodiimide dissociation is significantly lower with this combination than all other possibilities probed. The low barrier for azobenzene-bound Ti to dissociate an η^2-carbodiimide is a result of the azobenzene acting as a redox buffer, immediately accepting a pair of electrons upon dissociation of the η^2-carbodiimide and circumventing a discrete Ti^{II} intermediate. In addition, the unanticipated formation of the symmetrical carbodiimide ^{t}BuNCN^{t}Bu, a byproduct observed during catalysis, was proposed to form via a rare isocyanide metathesis mechanism evidenced through both experiment and DFT analysis. This is only the second report of an isocyanide metathesis in the literature. Importantly, this study indicates that certain substrates can participate in synergistic backbonding/redox buffering to significantly reduce the barrier for overall redox processes, which may provide further avenues for exploring early transition metal redox catalysis outside of more classical redox noninnocent ligand designs.

EXPERIMENTAL SECTION

General Considerations. All chemical manipulations were carried out in a glovebox under a nitrogen atmosphere. Azobenzene (TCI America) was purified *via* flash chromatography (hexanes), finely ground, and dried *in vacuo* prior to use. Substituted azobenzenes,[19,20] *tert*-butylisocyanide,[76] cyclohexylisocyanide,[77] 2,6-dimethylphenylisocyanide,[78] 1-*tert*-butyl-3-phenylcarbodiimide,[79] 1-(2,6-dimethylphenyl)-3-phenylcarbodiimide,[80] 1-cyclohexyl-3-phenylcarbodiimide,[80] and 1,3-diphenylcarbodiimide[80] were prepared following literature procedures. 2,6-Dimethylphenylisocyanide and 1-azidoadamantane (Millipore-Sigma) were dried *in vacuo* overnight prior to use, and stored at -35 °C in the glovebox. Liquid isocyanides and carbodiimides were freeze-pump-thaw degassed three times, brought into the glovebox, passed through activated basic alumina, and stored at -35 °C. $py_3TiCl_2(N^tBu)$[81] and $(THF)_3TiI_2(NPh)$[17] were prepared following literature procedures. C_6D_5Br was prepared according to literature procedure.[82] NMR solvents were dried over CaH_2, vacuum transferred, and then filtered through activated basic alumina. CH_2Cl_2, hexanes, pentane, THF, $C_6H_5CH_3$, and $PhCF_3$ were dried on a Pure Process Technology solvent purification system.

^{1}H, ^{13}C, and ^{19}F NMR spectra were recorded on Bruker Avance 400 MHz, Bruker Avance III 500 MHz, or Bruker Avance III HD 500 MHz spectrometers. Chemical shifts are reported with respect to residual protio-solvent impurity for ^{1}H (s, 7.26 ppm for $CHCl_3$; s, 7.16 ppm for C_6D_5H; s 7.30 for most deshielded shift for C_6D_4HBr), solvent carbons for ^{13}C (t, 77.16 ppm for $CDCl_3$; t 128.08 ppm for C_6D_6) and CF_3COOH for ^{19}F (s, -76.6 ppm in $CDCl_3$). No-D reactions in $PhCF_3$ were referenced to 1,3,5-$(OMe)_3C_6H_3$ (s, 6.13 ppm for C_6H_3). For quantification of product yields with respect to 1,3,5-$(OMe)_3C_6H_3$, spectra were collected at a delay time = 30, acquisition time = 5, and number of scans = 4. GC

chromatographs were collected on Agilent 7890B GC system equipped with the HP-5 column (30 m, 0.32 mm, 0.25 μm, 7 inch cage), an oxidation-methanation reactor (Polyarc® System, Activated Research Company) and a FID detector for quantitative carbon detection.[83,84] X-ray data were collected using a Bruker Photon II CMOS diffractometer for data collection at 100(2) K using Mo Kα radiation (normal parabolic mirrors). The data intensity was corrected for absorption and decay (SADABS).[85] Final cell constants were obtained from least-squares fits of all measured reflections and the structure was solved and refined using SHELXL-2014/7.39.[86] All non-hydrogen atoms were refined with anisotropic displacement parameters. Details regarding refined data and cell parameters are available in Table S1. CCDC entry 1923119 contains the supplementary crystallographic data for this paper. These data can be obtained free of charge via http://www.ccdc.cam.ac.uk/conts/retrieving.html, Cambridge Crystallographic Data Center, 12 Union Road, Cambridge CB2 1EZ, United Kingdom, fax: (+44) 1223-336-033, or e-mail:deposit@ccdc.cam.ac.uk.

Computational Details. Geometry optimizations were performed using the Gaussian09 program version e01.[87] Calculations were run using the restricted M06 functional[88] at the 6-311G(d,p) basis set[89] with a superfine grid, and the SMD solvation model[90] for $PhCF_3$ with ε = 9.18. Thermodynamic corrections were calculated with frequency analysis to be either minima (with no imaginary frequencies) or transition states (with one imaginary frequency) with temperature corrections at 388.15 K, and the removal of frequencies smaller than 50 cm^{-1}. The NBO calculations utilized the NBO 5.G[65,66] program. The procedure used in this study for generating the d orbital occupation numbers is outlined in Webster et. Al.[91] The IBOs were generated in MOLPRO[92] using the the restricted M06 functional[88] at the 6-311G(d,p) basis set[89] and where visualized using VMD 1.9.3.[93]

Synthesis of py_3TiBr_2(NPh) (1b). The title compound was prepared in similar fashion to py_3TiBr_2(N-*p*-tolyl).[94] $TiBr_4$ (1.09 g, 2.97 mmol, 1 equiv.) and 10 mL CH_2Cl_2 were added to a 20 mL scintillation vial containing a Teflon stirbar in an N_2 glovebox. $(TMS)_2NPh$ (0.704 g, 2.97 mmol, 1 equiv.) in 8 mL CH_2Cl_2 was then slowly added to the mixture. The reaction was sealed with a Teflon screw cap and stirred for 0.5 h at 60 °C, then at room temperature for 1.5 h. The reaction mixture precipitated at this point and was filtered on a sintered glass frit. The precipitate was rinsed with 20 mL hexanes and dried *in vacuo*. The solid was then dissolved using approximately 10 mL CH_2Cl_2 and 5 mL pyridine and stirred at room temperature for 0.5 h. Next, the resulting solution was filtered through Celite and rinsed with CH_2Cl_2 until the filtrate became colorless (approximately 50 mL). The filtrate was then layered with 40 mL hexanes and cooled to -35 °C overnight to afford **1b** as dark brown crystals. Upon rinsing the resulting complex with hexanes, a yellow-brown powder was obtained. The resulting powder was dried in vacuo at 40 °C for 2 days, affording 825 mg of **1b** (52%). Elemental analysis was not attempted, as complex decomposition through pyridine loss would occur under prolonged drying on the vacuum line. ^{1}H NMR (400 MHz, $CDCl_3$, 25 °C, δ, ppm): 9.13 (br s, 4H, py-*H*), 8.89 (br s, 2H, py-*H*), 7.83 (t, *J* = 7.2 Hz, 2H, py-*H*), 7.72 (br s, 1H, py-*H*), 7.36 (t, 4H, *J* = 6.2 Hz, py-*H*), 7.29 (br s, 2H, py-*H*), 7.07-7.08 (m, 4H, Ar-*H*), 6.82 (m, 1H, Ar-*H*). ^{13}C NMR (101 MHz, $CDCl_3$, 25 °C, δ, ppm): 152.1, 151.4, 138.9, 137.5, 124.2, 124.0, 122.7.

Synthesis of $[py_2TiBr_2(N^tBu)]_2$ (1d). $TiBr_4$ (3.00 g, 8.16 mmol, 1 equiv.) and 60 mL CH_2Cl_2 were added to a 200 mL round bottom flask containing a Teflon stir bar in an N_2 glove box. The flask was sealed with a rubber septum and cooled to -35 °C. Then, *tert*-butylamine (3.76 g, 51.4 mmol, 6.3 equiv.) was added slowly. The reaction was sealed with a rubber septum and allowed to stir at room temperature for 4 h. The reaction mixture was filtered over Celite to remove the resulting precipitate and rinsed with CH_2Cl_2 until the filtrate became colorless (approximately 50 mL). The filtrate was transferred to a clean 200 mL round bottom flask containing a Teflon stir-bar. Pyridine (2.65 g, 33.5 mmol, 4.1 equiv.) was then added, and the flask was sealed with a rubber septum and allowed to stir at room temperature overnight. Volatiles were removed *in vacuo*, and the reaction mixture was suspended in hot $PhCH_3$ (approximately 150 mL), filtered over Celite, and rinsed with additional hot $PhCH_3$ until the filtrate grew clear in color (approximately 150 mL). Volatiles were removed *in vacuo*, and the resulting solid was dissolved in minimal hot CH_2Cl_2, cooled to room temperature, then layered with an equal volume of hexane and allowed to cool to -35 °C for several days to afford 2.78 g of **1d** as an orange crystalline solid (78%). X-ray quality crystals were grown via vapor diffusion of pentane into a CH_2Cl_2 solution of **1d** at room temperature overnight. ^{1}H NMR (400 MHz, $CDCl_3$, 25 °C, δ, ppm): 9.31 (d, 4H, *J* = 4.9 Hz, py-*H*), 7.86 (t, 2H, *J* = 7.5 Hz, py-*H*), 7.43 (t, 4H, *J* = 6.5 Hz, py-*H*), 1.04 (s, 9H, -C(CH_3)$_3$). ^{13}C NMR (101 MHz, $CDCl_3$, 25 °C, δ, ppm): 152.1, 138.8, 124.1, 74.6, 30.6.

General Procedure for Reaction Optimization: 0.5 mL of a stock solution of $PhCF_3$ containing 0.330 M azobenzene (30.1 mg, 0.165 mmol), 0.729 M *tert*-butyl isocyanide (30.3 mg, 0.365 mmol), and 0.0326 M 1,3,5-$(OMe)_3C_6H_3$ (2.74 mg, 0.0163 mmol) as an internal standard was prepared and used for NMR tube reactions related to the reaction optimization reactions. In an N_2 glovebox, the requisite Ti catalyst (10 mol % in Ti, 0.0165 mmol in Ti) was added to an NMR tube and was dissolved with 0.5 mL of the stock solution. The NMR tube was sealed, then wrapped with electric tape and parafilm, and an initial t = 0 No-D NMR spectrum was taken. The reaction was then heated in an oil bath for 24 h at 115 °C. After 24 h, a final No-D NMR spectrum was taken. Yields were determined by referencing to the internal standard, 1,3,5-$(OMe)_3C_6H_3$.

General Procedure for Diazene Scope: 0.5 mL of a stock solution of C_6D_5Br containing 0.0165 M $[py_2TiBr_2(N^tBu)]_2$ (**1d**, 7.2 mg, 0.00824 mmol, 10 mol % in Ti), 0.986 M *tert*-butyl isocyanide (41.0 mg, 0.493 mmol), and 0.0359 M 1,3,5-$(OMe)_3C_6H_3$ (3.02 mg, 0.0180 mmol) as an internal standard was prepared and used for NMR tube reactions related to the diazene scope. In an N_2 glovebox, the requisite diazene (0.165 mmol) was added to an NMR tube and was

dissolved with 0.5 mL of the stock solution. The NMR tube was sealed, then wrapped with electric tape and parafilm, and an initial t = 0 ^{1}H NMR spectrum was taken. The reaction was then heated in an oil bath for 24 h at 115 °C. After 24 h, a final ^{1}H NMR spectrum was taken. Yields were determined by referencing to the internal standard, 1,3,5-$(OMe)_3C_6H_3$.

ASSOCIATED CONTENT

Supporting Information

The Supporting Information is available free of charge on the ACS Publications website.

Full experimental, kinetic, and computational details are provided in the supporting information (PDF).

AUTHOR INFORMATION

Corresponding Author

* (I.A.T.) E-mail: itonks@umn.edu

** (J.D.G.) E-mail: jgoodpas@umn.edu*

ACKNOWLEDGMENT

Financial support was provided by the National Institutes of Health (1R35GM119457), and the Alfred P. Sloan Foundation (I.A.T. is a 2017 Sloan Fellow). Instrumentation for the University of Minnesota Chemistry NMR facility was supported from a grant through the National Institutes of Health (S10OD011952). X-ray diffraction experiments were performed with a diffractometer purchased through a grant from NSF/MRI (1229400) and the University of Minnesota. We acknowledge the Minnesota Supercomputing Institute (MSI) at the University of Minnesota and the National Energy Research Scientific Computing Center (NERSC), a DOE Office of Science User Facility supported by the Office of Science of the U.S. Department of Energy under Contract No. DE-AC02-05CH11231, for providing resources that contributed to the results reported within this paper.

REFERENCES

(1) Müller, P.; Fruit, C. Enantioselective Catalytic Aziridinations and Asymmetric Nitrene Insertions into CH Bonds. *Chem. Rev.* **2003**, *103*, 2905–2919.

(2) Halfen, J. A. Recent Advances in Metal-Mediated Carbon-Nitrogen Bond Formation Reactions: Aziridination and Amidation. *Curr. Org. Chem.* **2005**, *9*, 657–669.

(3) Degennaro, L.; Trinchera, P.; Luisi, R. Recent Advances in the Stereoselective Synthesis of Aziridines. *Chem. Rev.* **2014**, *114*, 7881–7929.

(4) Zalatan, D. N.; Du Bois, J. Metal-Catalyzed Oxidations of C-H to C-N Bonds. *Top. Curr. Chem.* **2010**, *292*, 347–378.

(5) Kornecki, K. P.; Berry, J. F.; Powers, D. C.; Ritter, T. Metal-Metal Bond-Containing Complexes as Catalysts for C-H Functionalization. *Prog. Inorg. Chem.* **2014**, *58*, 225–302.

(6) Roizen, J. L.; Harvey, M. E.; Du Bois, J. Metal-Catalyzed Nitrogen-Atom Transfer Methods for the Oxidation of Aliphatic C-H Bonds. *Acc. Chem. Res.* **2012**, *45*, 911–922.

(7) Davies, H. M. L.; Manning, J. R. Catalytic C-H Functionalization by Metal Carbenoid and Nitrenoid Insertion. *Nature* **2008**, *451*, 417–424.

(8) Du Bois, J. Rhodium-Catalyzed C-H Amination. an Enabling Method for Chemical Synthesis. *Org. Process Res. Dev.* **2011**, *15*, 758–762.

(9) Alderson, J. M.; Corbin, J. R.; Schomaker, J. M. Tunable, Chemo- and Site-Selective Nitrene Transfer Reactions through the Rational Design of Silver(I) Catalysts. *Acc. Chem. Res.* **2017**, *50*, 2147–2158.

(10) Lu, H.; Zhang, X. P. Catalytic C-H Functionalization by Metalloporphyrins: Recent Developments and Future Directions. *Chem. Soc. Rev.* **2011**, *40*, 1899–1909.

(11) Che, C.-M.; Lo, V. K.-Y.; Zhou, C.-Y.; Huang, J.-S. Selective Functionalisation of Saturated C-H Bonds with Metalloporphyrin Catalysts. *Chem. Soc. Rev.* **2011**, *40*, 1950–1975.

(12) Fantauzzi, S.; Caselli, A.; Gallo, E. Nitrene Transfer Reactions Mediated by Metallo-Porphyrin Complexes. *Dalt. Trans.* **2009**, *0*, 5434–5443.

(13) Wolczanski, P. T. Activation of Carbon-Hydrogen Bonds via 1,2-RH-Addition/-Elimination to Early Transition Metal Imides. *Organometallics* **2018**, *37*, 505–516.

(14) Hazari, N.; Mountford, P. Reactions and Applications of Titanium Imido Complexes. *Acc. Chem. Res.* **2005**, *38*, 839–849.

(15) Müller, T. E.; Hultzsch, K. C.; Yus, M.; Foubelo, F.; Tada, M. Hydroamination: Direct Addition of Amines to Alkenes and Alkynes. *Chem. Rev.* **2008**, *108*, 3795–3892.

(16) Odom, A. L.; McDaniel, T. J. Titanium-Catalyzed Multicomponent Couplings: Efficient One-Pot Syntheses of Nitrogen Heterocycles. *Acc. Chem. Res.* **2015**, *48*, 2822–2833.

(17) Chiu, H. C.; Tonks, I. A. Trimethylsilyl-Protected Alkynes as Selective Cross-Coupling Partners in Titanium-Catalyzed [2+2+1] Pyrrole Synthesis. *Angew. Chemie - Int. Ed.* **2018**, *57*, 6090–6094.

(18) Davis-Gilbert, Z. W.; Yao, L. J.; Tonks, I. A. Ti-Catalyzed Multicomponent Oxidative Carboamination of Alkynes with Alkenes and

Diazenes. *J. Am. Chem. Soc.* **2016**, *138*, 14570–14573.

(19) Gilbert, Z. W.; Hue, R. J.; Tonks, I. A. Catalytic Formal [2+2+1] Synthesis of Pyrroles from Alkynes and Diazenes via TiII/TiIV Redox Catalysis. *Nat. Chem.* **2016**, *8*, 63–68.

(20) Davis-Gilbert, Z. W.; Wen, X.; Goodpaster, J. D.; Tonks, I. A. Mechanism of Ti-Catalyzed Oxidative Nitrene Transfer in [2 + 2 + 1] Pyrrole Synthesis from Alkynes and Azobenzene. *J. Am. Chem. Soc.* **2018**, *140*, 7267–7281.

(21) Davis-Gilbert, Z. W.; Kawakita, K.; Blechschmidt, D. R.; Tsurugi, H.; Mashima, K.; Tonks, I. A. In Situ Catalyst Generation and Benchtop-Compatible Entry Points for TiII/TiIV Redox Catalytic Reactions. *Organometallics* **2018**, *37*, 4439–4445.

(22) Davis-Gilbert, Z. W.; Tonks, I. A. Titanium Redox Catalysis: Insights and Applications of an Earth-Abundant Base Metal. *Dalt. Trans.* **2017**, *46*, 11522–11528.

(23) Chiu, H.-C.; See, X. Y.; Tonks, I. A. Dative Directing Group Effects in Ti-Catalyzed [2+2+1] Pyrrole Synthesis: Chemo- and Regioselective Alkyne Heterocoupling. *ACS Catal.* **2018**, *9*, 216–223.

(24) Beaumier, E. P.; Pearce, A. J.; See, X. Y.; Tonks, I. A. Modern Applications of Low-Valent Early Transition Metals in Synthesis and Catalysis. *Nat. Rev. Chem.* **2019**, *3*, 15–34.

(25) Bauminger, S.; Wilchek, M. The Use of Carbodiimides in the Preparation of Immunizing Conjugates. *Methods Enzymol.* **1980**, *70*, 151–159.

(26) Li, P.; Xu, J.-C. Highly Efficient Synthesis of Peptides by Rational Utilization of Novel Coupling Reagents. *Chin. J. Chem.* **2000**, *18*, 456–466.

(27) Albericio, F.; Bailén, M. A.; Chinchilla, R.; Dodsworth, D. J.; Nájera, C. New Trends in Peptide Coupling Reagents. *Org. Prep. Proced. Int.* **2001**, *33*, 203–313.

(28) Schmidt, C. L. Polycarbodiimides. *Russ. Chem. Rev.* **1993**, *62*, 1119–1138.

(29) Kennemur, J. G.; Novak, B. M. Advances in Polycarbodiimide Chemistry. *Polymer* **2011**, *52*, 1693–1710.

(30) Khorana, H. G. The Chemistry of Carbodiimides. *Chem. Rev.* **1953**, *53*, 145–166.

(31) Kurzer, F.; Douraghi-Zadeh, K. Advances in the Chemistry of Carbodiimides. *Chem. Rev.* **1967**, *67*, 107–152.

(32) Williams, A.; Ibrahim, I. T. Carbodiimide Chemistry: Recent Advances. *Chem. Rev.* **1981**, *81*, 589–636.

(33) Ulrich, H. *Chemistry and Technology of Carbodiimides*; John Wiley & Sons: Chichester, England, 2007.

(34) Stevens, C. L.; Singhal, G. H.; Ash, A. B. Carbodiimides. Dehydration of Ureas. *J. Org. Chem.* **1967**, *32*, 2895.

(35) Jászay, Z. M.; Petneházy, I.; Töke, L.; Szajáni, B. Preparation of Carbodiimides Using Phase-Transfer Catalysis. *Synthesis* **1987**, *1987*, 520–523.

(36) Mitsunobu, O.; Kato, K.; Tomari, M. Preparation of Carbodiimides by the Reaction of Thioureas with Diethyl Azodicarboxylate. *Tetrahedron* **1970**, *26*, 5731–5736.

(37) Kim, S.; Yi, K. Y. Di-2-Pyridyl Sulfite. A New Useful Reagent for the Preparation of N-Sulfinylamines, Nitriles, Isocyanides, and Carbodiimides under Mild Conditions. *Tetrahedron Lett.* **1986**, *27*, 1925–1928.

(38) Saegusa, T.; Ito, Y.; Shimizu, T. Synthetic Reactions by Complex Catalysts. XVIII. The Reaction of Azide with Isocyanide by Iron Carbonyl Catalyst. A New Route to Carbodiimide. *J. Org. Chem.* **1970**, *35*, 3995–3996.

(39) Cowley, R. E.; Eckert, N. A.; Elhaïk, J.; Holland, P. L. Catalytic Nitrene Transfer from an Imidoiron(III) Complex to Form Carbodiimides and Isocyanates. *Chem. Commun.* **2009**, 1760–1762.

(40) Cowley, R. E.; Golder, M. R.; Eckert, N. A.; Al-Afyouni, M. H.; Holland, P. L. Mechanism of Catalytic Nitrene Transfer Using Iron(I)-Isocyanide Complexes. *Organometallics* **2013**, *32*, 5289–5298.

(41) Mankad, N. P.; Mu, P.; Peters, J. C. Catalytic N - N Coupling of Aryl Azides To Yield Azoarenes via Trigonal Bipyramid Iron - Nitrene Intermediates. *J. Am Chem. Soc.* **2010**, *132*, 4083.

(42) Wiese, S.; Aguila, M. J. B.; Kogut, E.; Warren, T. H. β-Diketiminato Nickel Imides in Catalytic Nitrene Transfer To Isocyanides. *Organometallics* **2013**, *32*, 2300–2308.

(43) Laskowski, C. A.; Hillhouse, G. L. Group-Transfer Reactions of Ni(II) - Ni(II) Bridging Imido Complexes. Catalytic Formation of Carbodiimides and Isocyanates via Nitrene Transfer from Organoazides. *Organometallics* **2009**, *28*, 6114–6120.

(44) Yousif, M.; Tjapkes, D. J.; Lord, R. L.; Groysman, S. Catalytic Formation of Asymmetric

Carbodiimides at Mononuclear Chromium(II/IV) Bis(Alkoxide) Complexes. *Organometallics* **2015**, *34*, 5119–5128.

(45) Zhang, Z.; Li, Z.; Fu, B.; Zhang, Z. Palladium-Catalyzed Cross-Coupling Reaction of Azides with Isocyanides. *Chem. Commun.* **2015**, *51*, 16312–16315.

(46) Kriegel, B. M.; Bergman, R. G.; Arnold, J. Nitrene Metathesis and Catalytic Nitrene Transfer Promoted by Niobium Bis(Imido) Complexes. *J. Am. Chem. Soc.* **2016**, *138*, 52–55.

(47) Nguyen, A. I.; Zarkesh, R. A.; Lacy, D. C.; Thorson, M. K.; Heyduk, A. F. Catalytic Nitrene Transfer by a Zirconium(IV) Redox-Active Ligand Complex. *Chem. Sci.* **2011**, *2*, 166–169.

(48) Pathare, R. S.; Ansari, A. J.; Verma, S.; Maurya, A.; Maurya, A. K.; Agnihotri, V. K.; Sharon, A.; Pardasani, R. T.; Sawant, D. M. Sequential Pd(0)/Fe(III) Catalyzed Azide–Isocyanide Coupling/Cyclization Reaction: One-Pot Synthesis of Aminotetrazoles. *J. Org. Chem.* **2018**, *83*, 9530–9537.

(49) Ansari, A. J.; Pathare, R. S.; Maurya, A. K.; Agnihotri, V. K.; Khan, S.; Roy, T. K.; Sawant, D. M.; Pardasani, R. T. Synthesis of Diverse Nitrogen Heterocycles via Palladium-Catalyzed Tandem Azide–Isocyanide Cross-Coupling/Cyclization: Mechanistic Insight Using Experimental and Theoretical Studies. *Adv. Synth. Catal.* **2018**, *360*, 290–297.

(50) Zhang, Z.; Xiao, F.; Huang, B.; Hu, J.; Fu, B.; Zhang, Z. Cyclization of Alkyne − Azide with Isonitrile/CO via Self-Relay Rhodium Catalysis. *Org. Lett.* **2016**, *18*, 908–911.

(51) Chen, K.; Tang, X.-Y.; Shi, M. Rh(II)-Catalyzed Formation of Pyrrolo[2,3-b]Quinolines from Azide-Methylenecyclopropanes and Isonitriles. *Chem. Commun.* **2016**, *52*, 1967–1970.

(52) He, Y.; Yuan, C.; Jiang, Z.; Shuai, L.; Xiao, Q. Expeditious Synthesis of Isoquinolone Derivatives by Rhodium(I)-Catalyzed Annulation Reaction through C–C Bond Cleavage. *Org. Lett.* **2019**, *21*, 185–189.

(53) Walsh, P. J.; Hollander, F. J.; Bergman, R. G. Monomeric and Dimeric Zirconocene Imido Compounds: Synthesis, Structure, and Reactivity. *Organometallics* **1993**, *12*, 3705–3723.

(54) Dunn, S. C.; Hazari, N.; Cowley, A. R.; Green, J. C.; Mountford, P. Synthesis and Reactions of Group 4 Imido Complexes Supported by Cyclooctatetraene Ligands. *Organometallics* **2006**, *25*, 1755–1770.

(55) Royo, P.; Sánchez-Nieves, J. Oxo and Imido/Imido Exchange and C-H Activation Reactions Based on Pentamethylcyclopentadienyl Imido Tantalum Complexes. *J. Organomet. Chem.* **2000**, *597*, 61–68.

(56) Barnea, E.; Majumder, S.; Staples, R. J.; Odom, A. L. One-Step Route to 2,3-Diaminopyrroles Using a Titanium-Catalyzed Four-Component Coupling. *Organometallics* **2009**, *28*, 3876–3881.

(57) Aldrich, K. E.; Odom, A. L. Titanium-Catalyzed Hydroamination and Multicomponent Coupling with a Simple Silica-Supported Catalyst. *Organometallics* **2018**, *37*, 4341–4349.

(58) Heins, S. P.; Wolczanski, P. T.; Cundari, T. R.; MacMillan, S. N. Redox Non-Innocence Permits Catalytic Nitrene Carbonylation by (Dadi)Ti=NAd (Ad = Adamantyl). *Chem. Sci.* **2017**, *8*, 3410–3418.

(59) Hill, J. E.; Profilet, R. D.; Fanwick, P. E.; Rothwell, I. P. Synthesis, Structure, and Reactivity of Aryloxo(Imido)Titanium Complexes. *Angew. Chemie Int. Ed. English* **1990**, *29*, 664–665.

(60) Edema, J. J. H.; Duchateau, R.; Gambarotta, S.; Hynes, R.; Gabe, E. Novel Titanium(II) Amine Complexes L4TiCl2[L = 1/2 N,N,N',N'-Tetramethylethylenediamine (TMEDA), 1/2 N,N,N'-Trimethylethylenediamine, Pyridine, 1/2 2,2'-Bipyridine]: Synthesis and Crystal Structure of Monomeric Trans-(TMEDA)2TiCl2. *Inorg. Chem.* **1991**, *30*, 154–156.

(61) Gray, S. D.; Thorman, J. L.; Adamian, V. A.; Kadish, K. M.; Woo, L. K. Synthesis, Electrochemistry, and Imido Transfer Reactions of (TTP)Ti(η2-PhN=NPh). *Inorg. Chem.* **1998**, *37*, 1–4.

(62) Wijeratne, G. B.; Zolnhofer, E. M.; Fortier, S.; Grant, L. N.; Carroll, P. J.; Chen, C.-H.; Meyer, K.; Krzystek, J.; Ozarowski, A.; Jackson, T. A.; Mindiola, D. J.; Telser, J. Electronic Structure and Reactivity of a Well-Defined Mononuclear Complex of Ti(II). *Inorg. Chem.* **2015**, *54*, 10380–10397.

(63) Knizia, G.; Klein, J. E. M. N. Electron Flow in Reaction Mechanisms—Revealed from First Principles. *Angew. Chem. Int. Ed.* **2015**, *54*, 5518–5522.

(64) Knizia, G. Intrinsic Atomic Orbitals: An Unbiased Bridge between Quantum Theory and Chemical Concepts. *J. Chem. Theory Comput.* **2013**, *9*, 4834–4843.

(65) Glendening, E. D.; Landis, C. R.; Weinhold, F. NBO 6 . 0 : Natural Bond Orbital Analysis Program. *J. Comput. Chem.* **2013**, *34*, 1429–1437.

(66) Weinhold, F.; Landis, C. R. *Valency and Bonding: A Natural Bond Orbital Donor-Acceptor Perspective*; Cambridge University Press: Cambridge, 2005.

(67) Guo, J.; Deng, X.; Song, C.; Lu, Y.; Qu, S.; Dang, Y.; Wang, Z.-X. Differences between the Elimination of Early and Late Transition Metals: DFT Mechanistic Insights into the Titanium-Catalyzed Synthesis of Pyrroles from Alkynes and Diazenes. *Chem. Sci.* **2017**, *8*, 2413–2425.

(68) Guo, J.; Lu, Y.; Zhao, R.; Liu, Z.; Menberu, W.; Wang, Z.-X. Strong Preference of the Redox-Neutral Mechanism over the Redox Mechanism for the TiIV Catalysis Involved in the Carboamination of Alkyne with Alkene and Diazene. *Chem. Eur. J.* **2018**, *24*, 7010–7025.

(69) Zuckerman, R. L.; Bergman, R. G. Structural Factors That Influence the Course of Overall [2 + 2] Cycloaddition Reactions between Imidozirconocene Complexes and Heterocumulenes. *Organometallics* **2000**, *19*, 4795–4809.

(70) Zuckerman, R. L.; Bergman, R. G. Mechanistic Investigation of Cycloreversion/Cycloaddition Reactions between Zirconocene Metallacycle Complexes and Unsaturated Organic Substrates. *Organometallics* **2001**, *20*, 1792–1807.

(71) Guiducci, A. E.; Boyd, C. L.; Mountford, P. Reactions of Cyclopentadienyl-Amidinate Titanium Imido Compounds with CS2, COS, Isocyanates, and Other Unsaturated Organic Compounds. *Organometallics* **2006**, *25*, 1167–1187.

(72) Meisel, I.; Hertel, G.; Weiss, K. Investigations of Polymerizations and Metathesis Reactions Part IX. Metathesis of Carbodiimides with Tungsten(VI)-Imido Complexes. *J. Mol. Catal.* **1986**, *36*, 159–162.

(73) Birdwhistell, K. R.; Lanza, J.; Pasos, J. Carbodiimide Metathesis Catalyzed by Vanadium Oxo and Imido Complexes via Imido Transfer. *J. Organomet. Chem.* **1999**, *584*, 200–205.

(74) Ong, T.-G.; Yap, G. P. A.; Richeson, D. S. Catalytic C=N Bond Metathesis of Carbodiimides by Group 4 and 5 Imido Complexes Supported by Guanidinate Ligands. *Chem. Commun.* **2003**, *0*, 2612–2613.

(75) Louie, J. Transition Metal Catalyzed Reactions of Carbon Dioxide and Other Heterocumulenes. *Curr. Org. Chem.* **2005**, *9*, 605–623.

(76) Gokel, G. W.; Widera, R. P.; Weber, W. P. Phase-Transfer Hofmann Carbylamine Reaction: Tert-Butyl Isocyanide. *Org. Synth.* **1976**, *55*, 96.

(77) Ugi, I.; Meyr, R.; Lipinski, M.; Bodesheim, F.; Rosendahl, F. Cyclohexyl Isocyanide. *Org. Synth.* **1961**, *41*, 13.

(78) Li, J.; Wang, N.; Li, C.; Jia, X. Multicomponent Reaction to Construct Spirocyclic Oxindoles with a Michael (Triple Michael)/Cyclization Cascade Sequence as the Key Step. *Chem. Eur. J.* **2012**, *18*, 9645–9650.

(79) Yoshiizumi, K.; Ikeda, S.; Goto, K.; Morita, T.; Nishimura, N.; Sukamoto, T.; Yoshino, K. Synthesis and Structure-Activity Relationships of Novel Phenylcyanoguanidine Derivatives as Potassium Channel Openers. *Chem. Pharm. Bull.* **1996**, *44*, 2042–2050.

(80) Ali, A. R.; Ghosh, H.; Patel, B. K. A Greener Synthetic Protocol for the Preparation of Carbodiimide. *Tetrahedron Lett.* **2010**, *51*, 1019–1021.

(81) Blake, A. J.; Collier, P. E.; Dunn, S. C.; Li, W.-S.; Mountford, P.; Shishkin, O. V. Synthesis and Imido-Group Exchange Reactions of Tert-Butylimidotitanium Complexes. *J. Chem. Soc., Dalt. Trans.* **1997**, *0*, 1549–1558.

(82) Whitesides, G. M.; Ehmann, W. J. The Mechanism of Formation of 1,2,3,4-Tetramethylnaphthalene from 2-Butyne and Triphenyltris(Tetrahydrofuran)Chromium(III). *J. Am Chem. Soc.* **1970**, *92*, 5625–5640.

(83) Beach, C. A.; Joseph, K. E.; Dauenhauer, P. J.; Spanjers, C. S.; Jones, A. J.; Mountziaris, Triantafillos, J. Complete Carbon Analysis of Sulfur-Containing Mixtures Using Postcolumn Reaction and Flame Ionization Detection. *AIChE J.* **2017**, *63*, 5438–5444.

(84) Spanjers, C. S.; Beach, C. A.; Jones, A. J.; Dauenhauer, P. J. Increasing Flame Ionization Detector (FID) Sensitivity Using Post-Column Oxidation-Methanation. *Anal. Methods* **2017**, *9*, 1928–1934.

(85) Blessing, R. H. An Empirical Correction for Absorption Anisotropy. *Acta Crystallogr., Sect. A* **1995**, *51*, 33–38.

(86) Sheldrick, G. M. SHELXT - Integrated Space-Group and Crystal-Structure Determination. *Acta Crystallogr., Sect. A* **2015**, *71*, 3–8.

(87) Frisch, M. J.; Trucks, G. W.; Schlegel, H. B.; Scuseria, G. E.; Robb, M. A.; Cheeseman, J. R.; Scalmani, G.; Barone, V.; Mennucci, B.; Petersson, G. A.; Nakatsuji, H.; Caricato, M.; Li, X.; Hratchian, H. P.; Izmaylov, A. F.; Bloino, J.; Zheng, G.; Sonnenberg, J. L.; Hada, M.; Ehara, M.; Toyota, K.; Fukuda, R.; Hasegawa, J.; Ishida, M.; Nakajima, T.;

Honda, Y.; Kitao, O.; Nakai, H.; Vreven, T.; Montgomery, J. A., Jr.; Peralta, J. E.; Ogliaro, F.; Bearpark, M.; Heyd, J. J.; Brothers, E.; Kudin, K. N.; Staroverov, V. N.; Kobayashi, R.; Normand, J.; Raghavachari, K.; Rendell, A.; Burant, J. C.; Iyengar, S. S.; Tomasi, J.; Cossi, M.; Rega, N.; Millam, J. M.; Klene, M.; Knox, J. E.; Cross, J. B.; Bakken, V.; Adamo, C.; Jaramillo, J.; Gomperts, R.; Stratmann, R. E.; Yazyev, O.; Austin, A. J.; Cammi, R.; Pomelli, C.; Ochterski, J. W.; Martin, R. L.; Morokuma, K.; Zakrzewski, V. G.; Voth, G. A.; Salvador, P.; Dannenberg, J. J.; Dapprich, S.; Daniels, A. D.; Farkas, O.; Foresman, J. B.; Ortiz, J. V.; Cioslowski, J.; Fox, D. J. Gaussian 09, Revision B.01. Wallingford, CT 2008.

(88) Zhao, Y.; Truhlar, D. G. The M06 Suite of Density Functionals for Main Group Thermochemistry, Thermochemical Kinetics, Noncovalent Interactions, Excited States, and Transition Elements: Two New Functionals and Systematic Testing of Four M06-Class Functionals and 12 Other Function. *Theor. Chem. Acc.* **2008**, *120*, 215–241.

(89) Krishnan, R.; Binkley, J. S.; Seeger, R.; Pople, J. A. Self-Consistent Molecular Orbital Methods. XX. A Basis Set for Correlated Wave Functions. *J. Chem. Phys.* **1980**, *72*, 650–654.

(90) Marenich, A. V; Cramer, C. J.; Truhlar, D. G. Universal Solvation Model Based on Solute Electron Density and on a Continuum Model of the Solvent Defined by the Bulk Dielectric Constant and Atomic Surface Tensions. *J. Phys. Chem. B.* **2009**, *113*, 6378–6396.

(91) Webster, A. J.; Mueller, C. M.; Foegen, N. P.; Sit, P. H.-L.; Speetzen, E. D.; Cunningham, D. W.; D'Acchioli, J. S. Oxidation States ''naturally": A Natural Bond Orbital Method for Determining Transition Metal Oxidation States. *Polyhedron* **2016**, *114*, 128–132.

(92) Werner, H.-J.; Knowles, P. J.; Knizia, G.; Manby, F. R.; Schütz, M. Molpro: A General-Purpose Quantum Chemistry Program Package. *WIREs Comput. Mol. Sci.* **2012**, *2*, 242–253.

(93) Humphrey, W.; Dalke, A.; Schulten, K. VMD: Visual Molecular Dynamics. *J. Mol. Graph.* **1996**, *14*, 33–38.

(94) See, X. Y.; Beaumier, E. P.; Davis-Gilbert, Z. W.; Dunn, P. L.; Larsen, J. A.; Pearce, A. J.; Wheeler, T. A.; Tonks, I. A. Generation of TiII Alkyne Trimerization Catalysts in the Absence of Strong Metal Reductants. *Organometallics* **2017**, *36*, 1383–1390.

Table of Contents artwork